

HOSTED BY

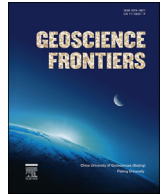


ELSEVIER

Contents lists available at ScienceDirect

China University of Geosciences (Beijing)

Geoscience Frontiers

journal homepage: [www.elsevier.com/locate/gsf](http://www.elsevier.com/locate/gsf)

## Research Paper

## Age and metal source of orogenic gold deposits in Southeast Guizhou Province, China: Constraints from Re–Os and He–Ar isotopic evidence

Jiasheng Wang<sup>a,b,\*</sup>, Hanjie Wen<sup>b</sup>, Chao Li<sup>c</sup>, Jinrang Zhang<sup>b</sup>, Wei Ding<sup>b</sup><sup>a</sup> Southwest Institute of Geological Survey, Kunming University of Science and Technology, Kunming 650093, China<sup>b</sup> State Key Laboratory of Ore Deposit Geochemistry, Institute of Geochemistry, Chinese Academy of Sciences, Guiyang 550002, China<sup>c</sup> National Research Center for Geoanalysis, Beijing 100037, China

## ARTICLE INFO

## Article history:

Received 22 December 2017

Received in revised form

4 April 2018

Accepted 24 May 2018

Available online xxx

Handling Editor: Stijn Glorie

## Keywords:

Re–Os geochronology

Arsenopyrite

He–Ar isotopes

Pingqiu

Jinjing

Southeast Guizhou Province, China

## ABSTRACT

The orogenic gold deposits in Southeast Guizhou are an important component of the Xuefeng poly-metallic ore belt and have significant exploration potential, but geochronology research on these gold deposits is scarce. Therefore, the ore genetic models are poorly constrained and remain unclear. In the present study, two important deposits (Pingqiu and Jinjing) are investigated, including combined Re–Os dating and the He–Ar isotope study of auriferous arsenopyrites. It is found that the arsenopyrites from the Pingqiu gold deposit yielded an isochron age of  $400 \pm 24$  Ma, with an initial  $^{187}\text{Os}/^{188}\text{Os}$  ratio of  $1.24 \pm 0.57$  (MSWD = 0.96). An identical isochron age of  $400 \pm 11$  Ma with an initial  $^{187}\text{Os}/^{188}\text{Os}$  ratio of  $1.55 \pm 0.14$  (MSWD = 0.34) was obtained from the Jinjing deposit. These ages correspond to the regional Caledonian orogeny and are interpreted to represent the age of the main stage ore. Both initial  $^{187}\text{Os}$  ratios suggest that the Os was derived from crustal rocks. Combined with previous rare earth element (REE), trace elements, Nd–Sr–S–Pb isotope studies on scheelite, inclusion fluids with other residues of gangue quartz, and sulfides from other gold deposits in the region, it is suggested that the ore metals from Pingqiu and Jinjing were sourced from the Xiajiang Group. The He and Ar isotopes of arsenopyrites are characterized by  $^3\text{He}/^4\text{He}$  ratios ranging from  $5.3 \times 10^{-4}$  Ra to  $2.5 \times 10^{-2}$  Ra ( $\text{Ra} = 1.4 \times 10^{-6}$ , the  $^3\text{He}/^4\text{He}$  ratio of air),  $^{40}\text{Ar}/^4\text{He}$  ratios from  $0.64 \times 10^{-2}$  to  $15.39 \times 10^{-2}$ , and  $^{40}\text{Ar}/^{36}\text{Ar}$  ratios from 633.2 to 6582.0. Those noble gas isotopic compositions of fluid inclusions also support a crustal source origin, evidenced by the Os isotope. Meanwhile, recent noble gas studies suggest that the amount of in situ radiogenic  $^4\text{He}$  generated should not be ignored, even when Th and U are present at levels of only a few ppm in host minerals.

© 2018, China University of Geosciences (Beijing) and Peking University. Production and hosting by Elsevier B.V. This is an open access article under the CC BY-NC-ND license (<http://creativecommons.org/licenses/by-nc-nd/4.0/>).

## 1. Introduction

The Xuefeng region, which corresponds to the southwest section of the Jiannan Orogenic Belt, is one of the most significant turbidite-hosted gold metallogenic belts in South China (Fig. 1). The region contains 319 gold deposits and occurrences (Peng and Dai, 1998), with a total reserve of >200 t. These gold deposits bear many similarities in terms of host rocks, structural style, and mineralization

style to other Proterozoic–Paleozoic turbidite-hosted gold deposits worldwide, such as the Hill End gold field in central New South Wales, Australia (Windh, 1995), the Bendigo–Ballarat gold zone in central Victoria, Australia (Arne et al., 2001), and the Meguma terrane gold field in Nova Scotia, Canada (Morelli et al., 2005). This type of turbidite-hosted gold deposits has been widely considered as one of the most important components of orogenic gold deposits (Groves et al., 1998; Goldfarb et al., 2001). Although extensively studied, the mineralization ages and the origin of ore fluids of these gold deposits are poorly constrained. To date, reported mineralization ages tend to be concentrated in the Caledonian (450–370 Ma) (Wang et al., 1999; Lu et al., 2005, 2006; Zhu et al., 2006), with very few in the Indosinian–Yanshanian (240–140 Ma) (Liu, 1993; Peng

\* Corresponding author. Southwest Institute of Geological Survey, Kunming University of Science and Technology, Kunming 650093, China.

E-mail address: [jiashengwang@126.com](mailto:jiashengwang@126.com) (J. Wang).

Peer-review under responsibility of China University of Geosciences (Beijing).

<https://doi.org/10.1016/j.gsf.2018.05.012>

1674–9871/© 2018, China University of Geosciences (Beijing) and Peking University. Production and hosting by Elsevier B.V. This is an open access article under the CC BY-NC-ND license (<http://creativecommons.org/licenses/by-nc-nd/4.0/>).

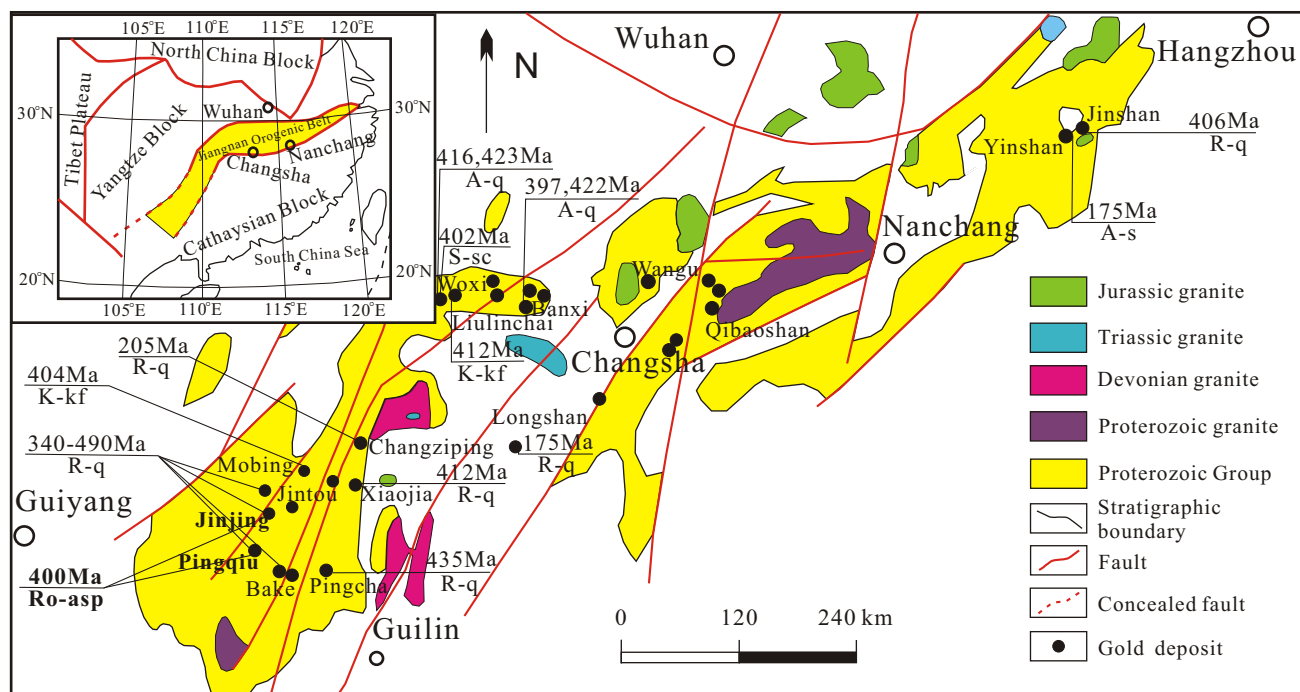


**Figure 1.** Simplified geologic map of the Jiangnan Orogenic Belt, showing reported ore-forming ages of major gold deposits. These ages were collated from Shi et al. (1993), Peng and Dai (1998), Wang et al. (1999), Peng and Frei (2004), Li et al. (2006, 2008), and Zhu et al. (2006). Test methods: A—Ar—Ar, K—K—Ar, R—Rb—Sr, S—Sm—Nd, Ro—Re—Os. Test samples: kf—K-feldspar, q—Quartz, sc—scheelite, s—Sericite, asp—arsenopyrite.

and Dai, 1998) and only one referenced Pb model age in the Wulin–Xuefeng period (1000–800 Ma) (Luo, 1989) for the gold deposits within the Jiangnan Orogenic Belt (Fig. 1). However, the Pb model age most likely reflects the sedimentary age of strata rather than the ore-forming age (Liu, 1993). Most of the reported Caledonian–Yanshanian ages were dated by gangue minerals such as K-feldspar, quartz and sericite, but in these isotopic studies (Rb–Sr, Sm–Nd, and U–Th–Pb) of spatially associated gangue minerals or wall-rock alterations, it is not always obvious how these minerals relate to ore formation (Freydier et al., 1997).

Pingqiu and Jinjing are the most significant deposits in the southwestern portion of the Xuefeng gold metallogenic belt, with no ore-related intrusions cropping out directly into or near the deposits. Zhu et al. (2006) reported ore-forming ages of 492–340 Ma for the gold deposits in Southeast Guizhou based on the Rb–Sr chronology of quartz fluid inclusions; in particular, ages of 492–477 Ma ( $492 \pm 37$  Ma;  $477 \pm 14$  Ma) and  $340 \pm 16$  Ma were obtained for the Pingqiu and Jinjing gold deposits, respectively, and  $430 \pm 44$  Ma and  $425 \pm 16$  Ma for the Jintou and Tonggu gold deposits, respectively. However, the five ages obtained by Zhu et al. (2006) are separated by large intervals and contain significant errors, suggesting that the data may provide inaccurate geochronological information for the mineralization. Accordingly, there is a demand, as a matter of necessity and potential, for the determination of the ages of the gold mineralization events of the Southeast Guizhou region in more detail.

Recently, Re–Os geochronology has been successfully applied to sulfides such as arsenopyrite (Arne et al., 2001; Mikulski et al., 2005; Morelli et al., 2005, 2007; Chen et al., 2015), pyrite (Stein et al., 1998; Mathur et al., 1999; Morelli et al., 2004; Zhang et al., 2005; Cardon et al., 2008; Feng et al., 2009; Hnatyshin et al., 2015; Li et al., 2016, 2017a), chalcopyrite (Freydier et al., 1997; Stein et al., 2000; Barra et al., 2003; Deng et al., 2016a), bornite and chalcocite (Selby et al., 2009), and molybdenite (Stein et al., 1998; Mao et al., 1999; Deng et al., 2013, 2016b; Li et al., 2017b).

These new developments in research demonstrate the potential to constrain the geochronology of medium-to low-temperature ore deposits by Re–Os geochronology. Stein et al. (1998) indicated that the Re–Os method is one of the most reliable isotopic dating tools that can directly date ore minerals because it is based on two siderophile–chalcophile sulfide-forming elements. In previous studies, the Re–Os geochronology of arsenopyrite had not been adopted as widely as that of molybdenite, owing primarily to the low Re and Os concentrations typical of arsenopyrite. Nevertheless, several significant ages have been obtained in various types of ore deposits since the potential of the Re–Os chronometry of arsenopyrite was first recognized by Frei et al. (1998). In addition, several reports suggested that Re–Os arsenopyrite chronometry may be widely applicable for orogenic gold deposits (Arne et al., 2001; Morelli et al., 2005, 2007). Furthermore, determination of the initial  $^{187}\text{Os}/^{188}\text{Os}$  ratio ( $\text{Os}_i$ ) is equally important in understanding ore genesis, as it provides evidence for the source of metals (Ruiz and Mathur, 1999).

Noble gases, especially He and Ar abundances and their isotopic composition analyses, have been applied to a variety of ore deposit types, mainly including orogenic gold deposits (Hu et al., 2004; Morelli et al., 2007; Zhu and Pen, 2015), porphyry copper deposits (Kendrick et al., 2001), and other hydrothermal deposits such as uranium deposits (Hu et al., 2009). Sulfide minerals (including pyrite, arsenopyrite, chalcopyrite, stibnite and etc.) are the most suitable traps for noble gases; despite a partial loss of trapped noble gases, He and Ar isotope ratios typically remain unchanged (Ballentine and Burnard, 2002; Hu et al., 2004). Morelli et al. (2007) found that Re–Os combined with He isotope analyses in arsenopyrite should provide valuable constraints for the origin of orogenic gold deposits worldwide.

In the gold deposits of the Xuefeng region, arsenopyrite, pyrite, galena, and sphalerite are the main gold-bearing minerals. According to Bao (1991), the relative gold abundances of each sulfide mineral, in decreasing order, are as follows: arsenopyrite > pyrite > (sphalerite)

galena. Despite pyrite being widely studied as the primary gold-bearing mineral, in some cases, arsenopyrite is more suitable for Re–Os dating because pyrite may be zoned and thus formed through a variety of different events (Chen et al., 2015). The Re–Os system of sphalerite (galena) may be disturbed by tectonic activities, and experimental results for such a Re–Os geochronology have been unreliable (Morelli et al., 2004). In contrast, the Re–Os system of arsenopyrite is relatively stable, and arsenopyrite is distributed dominantly in both gold deposits, especially in Jinjing, while other sulfides are scarce. Therefore, arsenopyrite Re–Os geochronology is currently considered as the most suitable direct dating method in the study area. In this context, the present study reveals the results of the Re–Os and He–Ar isotopic investigations of arsenopyrite from the Pingqiu and Jinjing gold deposits, and yields implications in the ages of mineralization, the origin of ore metals and fluids, and the geodynamic setting.

## 2. Geological setting

### 2.1. Regional geology

The Jiangnan Orogenic Belt in China stretches for 1500 km from northern Guangxi in the southwest to western Zhejiang in the east (Xue et al., 2010; Goldfarb et al., 2014; Deng et al., 2016). This belt contains Neoproterozoic epimetamorphic sedimentary turbidite and a series of igneous rocks, exhibiting a zoned distribution between the Yangtze and Cathaysia blocks (Fig. 1). It can be divided

into four gold districts: the northeastern Jiangxi district, the eastern Hunan–western Jiangxi district, the western Hunan district and the southeastern Guizhou–northern Guangxi district. The latter two districts represent the main part of the Xuefeng gold metallogenetic belt. The gold deposits in the Tianzhu–Jinping area, Southeast Guizhou, belong to the southwest section of this belt (Fig. 2). The stratigraphy of the area includes the Presinian Xiajiang Group (the equivalent of the Banxi Group in Hunan Province) and Sinian, Carboniferous, Permian, Jurassic, Cretaceous, and Quaternary units (Fig. 3). An angular unconformity exists between the Xiajiang Group and the other strata, and two parallel unconformities exist between the Carboniferous and Permian and between the Permian and Jurassic (Lu et al., 2005). The Xiajiang Group, up to 7 km thick, has been subdivided as follows (Fig. 3): the Fanzhao, Qingshuijiang, Pinglue, and Longli formations. Gold-bearing quartz veins are found in all of these formations, except the Pinglue Formation (Lu et al., 2005).

The Southeast Guizhou area has experienced multistage tectonic events since the Proterozoic (Lu et al., 2005). The NE–SW-trending tectonic framework was first established by the Xuefeng movement (1000–800 Ma, corresponding to Jinning Orogeny; Ren, 1996; Zhou et al., 2002; Pirajno, 2013; Goldfarb et al., 2014). Subsequently, several EW-trending shear zones were developed in association with the Caledonian movement (513–386 Ma; Ren, 1996; Zhou et al., 2002; Wang et al., 2007; Pirajno, 2013; Goldfarb et al., 2014), including the Gaoniang and Qimeng shear zones in the north and south of the study area, respectively. These

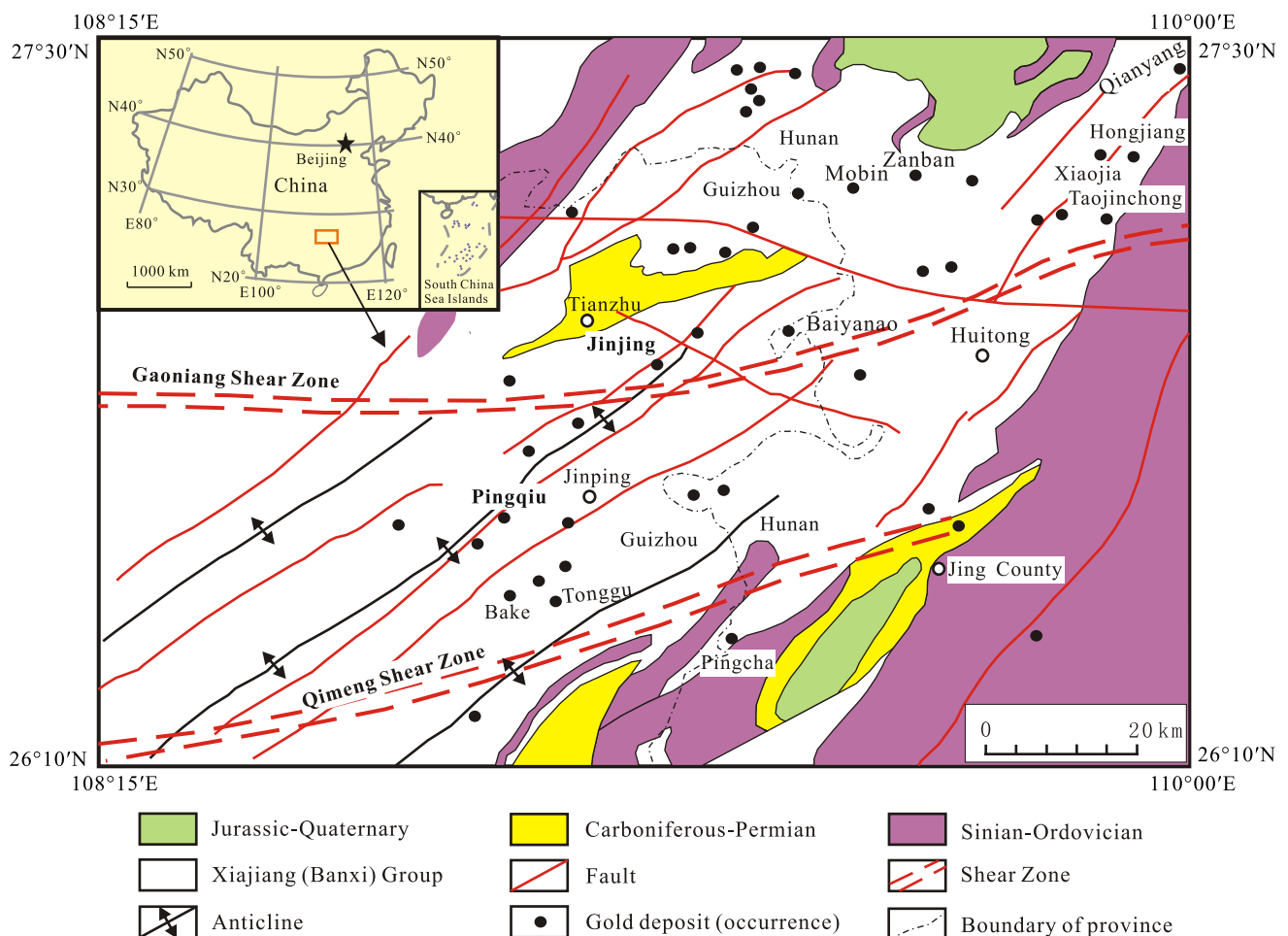


Figure 2. Geological map of SE Guizhou and west Hunan gold districts (modified from Lu et al., 2006).

Age	Formation	Histogram	Thickness (m)	Description	
Quaternary			<100	Soil	
Permian			<100	Limestone	
Carboniferous			<100	Dolomite, limestone	
Cambrian			<100	Black shale	
Sinian			300 — 1500	Blast-quartz sandstone, blast-pebbly sandstone, anagenite, graywacke, siltstone, black shale	
	Presinian	Longli	Second Section		700 — 900
First Section				600 — 800	Light grey-grey blastopsammite interbedded with slate, containing gold-bearing quartz
Pinglue				1500 — 2000	Slate with slight gray-celadon color and interbedded with a small amount of blastopsammite
			Qingshuijiang	Second Section	
First Section				1500 — 2000	Slight gray-celadon-charcoal grey palimpsest tuff, palimpsest tuffite and blastopsammite interbedded with slate, containing gold-bearing quartz
Fanzhao			>1000	Slate with gray-slight green color, interlayer with a small amount of blastopsammites, and palimpsest tuffs, containing gold-bearing quartz	

Figure 3. Stratigraphic column of SE Guizhou (modified from Lu et al., 2006).

two EW-trending shear zones controlled the graben-type structure and local subsidence in the Hercynian–Indosinian movements (386–205 Ma; Ren, 1996; Zhou et al., 2002; Wang et al., 2005; Pirajno, 2013). Both of these shear zones are basement fault zone, more than 50 km long, and characterized by multi-periodic activity (Lu et al., 2005), with fault displacement reaching up to 200–300 m. Many secondary structures (e.g., anticlines and faults) closely associated with mineralization have developed along these two shear zones where many gold deposits have formed, including the following: the Jinjing, Pingzao, Xiata, Xianggongtang, and Zhushanchong gold deposits in the Gaoniang shear zone; and the Tonggu, Dicha, Dichou, and Zhongling deposits, among others, in the Qimeng shear zone. During the Yanshanian movements (180–65 Ma; Ren, 1996; Zhou et al., 2002; Hu and Zhou, 2012; Mao et al., 2013; Pirajno, 2013), the overlapped N–NW-trending structures were formed, overprinting the EW-trending and NE-trending structures, and experienced sinistral transpressional shear due to the oblique subduction of the Pacific Plate under the Asian

continental plates. There are four main periods of granitic intrusions in the whole Jiangnan Orogenic Belt, which correspond to the four above tectonic events, the Proterozoic, Devonian, Triassic and Jurassic (Fig. 1), but only few are spatially related to gold mineralization, and magmatic rocks are absent in the study area.

## 2.2. Geologic characteristics of the Pingqiu and Jinjing gold deposits

The stratigraphy in the Pingqiu deposit area corresponds to the second section of the Fanzhao Formation and is mainly composed of greenschist facies metamorphic turbidite; this section is characterized by chlorite-sericite slate, silty slate, and blasto-psammites with lamellar and banded structures, and locally with inter-bedded palimpsest tuffaceous slate and vitric tuff. The NE-trending fold and fault are the dominant structures in this region. The EW-trending brittle fracture zones and interlayer sliding fault extending along the axial part of the anticline can be considered as secondary structures. The NE-trending structures are primarily represented by

the Taoziao, Daiou, and Jinchangxi anticlines and the reverse faults of F1 and F2; these are the dominant ore-controlling structures (Fig. 4). The gold-bearing quartz veins are well developed in the limbs, hinge zone, and axial parts of both the primary and secondary anticlines. There are two main types of veins: bedding-concordant and bedding-discordant veins. The former refers to quartz veins filling in intra-formational faults, where the ore bodies usually occur as stratiform, stratoid, saddle reef, or lenticular bodies, typically 0.10–1.05 m thick, 100–500 m long in the horizontal direction, and extending 50–100 m in the dip direction. Economic gold mineralization primarily occurs within narrow, laminated, bedding-parallel veins. Veins thicken into saddle reefs at anticlinal crests, but they generally only contain economic gold on fold limbs adjacent to the saddles. These characteristics look like typical saddle reefs and related gold mineralization worldwide, including the Bendigo-Ballarat zone, the Meguma terrane, and the Hill End gold field (Windh, 1995; Arne et al., 2001; Morelli et al., 2005). The grade of gold ranges from 0.50 g/t to 4.0 g/t, but as much as 96.0 g/t. The latter (bedding-discordant vein) type exhibits much more complex, which contains the textures with fault gouge, and brecciated vein fragments or wall rocks with lower gold grades. The ore bodies typically are tabular or lenticular, normally 1.63–2.56 m thick. The grade of the gold here ranges from 3.97 g/t to 4.38 g/t. Hydrothermal alteration is relatively weak on both the footwall and hanging walls of the ore-bearing quartz veins (<0.5 m), and mainly includes silicification, arsenopyritization,

pyritization, sericitization and Fe-dolomitization. The majority of metallic minerals are arsenopyrite, pyrite, sphalerite, galena, chalcocopyrite and native gold, compared with gangue minerals that are composed of quartz and ferrodolomite.

The stratigraphy in the Jinjing area can be considered as a member of the Qingshuijiang Formation of the Xiajiang Group; this stratigraphy is represented by light gray–celadon–charcoal gray palimpsest tuff, palimpsest tuffite and blasto-psammite inter bedded with slate, tuffaceous slate, and silty slate and is 1000 m thick. The dominant fold in the ore district is the NE-trending Jinjing anticline. From the axial part to both wings of this anticline, many inter-formational sliding zones and gaps exist, where quartz veins and gold ore bodies are likely to be abundant. The faults are primarily NE-, NW-, and EW-trending. The EW-trending is the dominant ore conducting structure in the ore district, and it extends along the axial part of the anticline as a secondary structure. There are almost 20 quartz veins in the study area, in which M6, M7, M10, M11, M19, M20, and M21 are the dominant gold-bearing veins (Fig. 5). The ore bodies typically occur as bedding-parallel veins, approximately 0.2–1.45 m thick, 400–800 m long in the horizontal direction, and extending for 150–300 m in the dip direction. The orebody characteristics in Jinjing are in good agreement with those of saddle reefs in Pingqiu, the Bendigo-Ballarat zone, the Meguma terrane, and the aforementioned Hill End gold field (Windh, 1995; Arne et al., 2001; Morelli et al., 2005). The grade of gold ranges from 4.85 g/t to

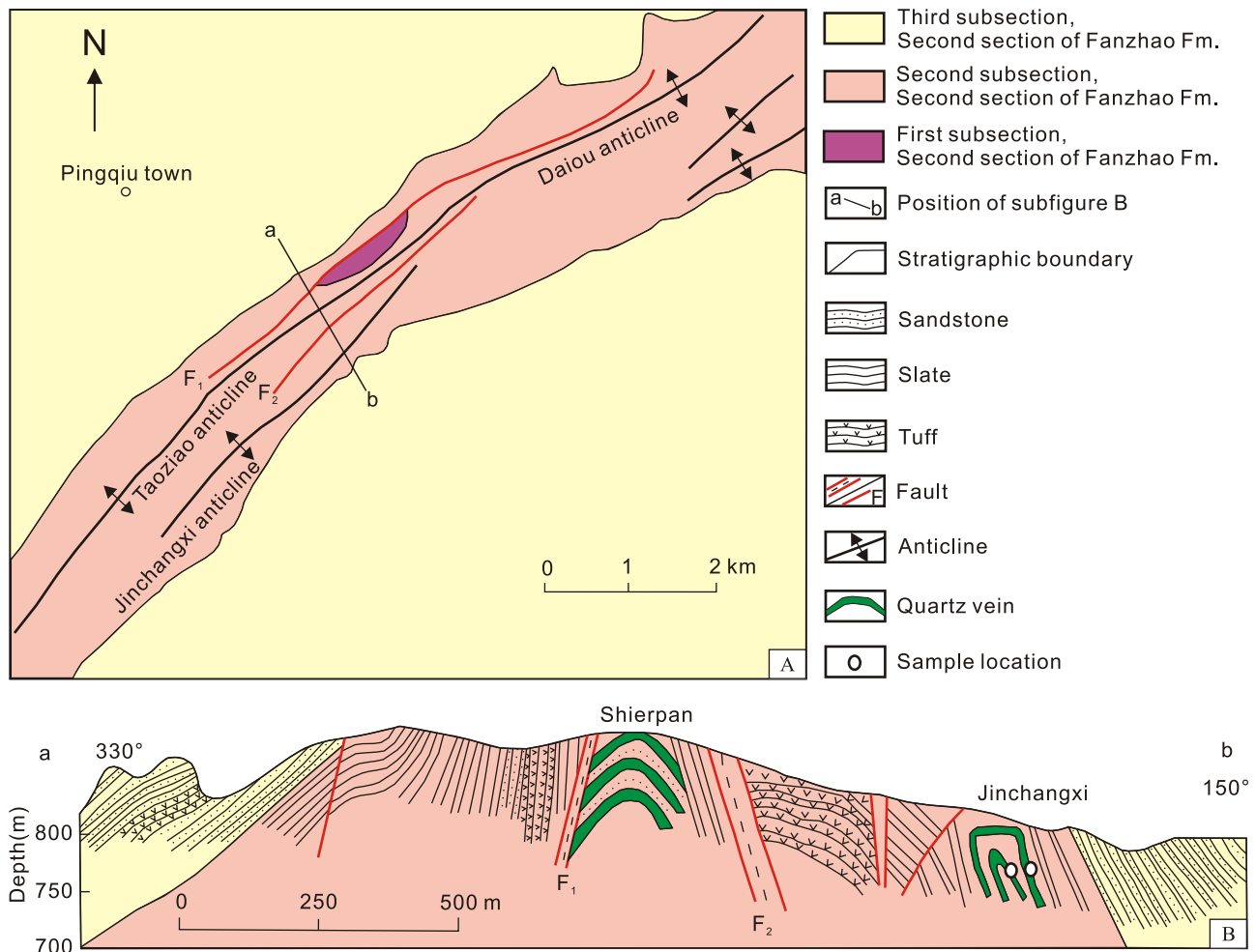
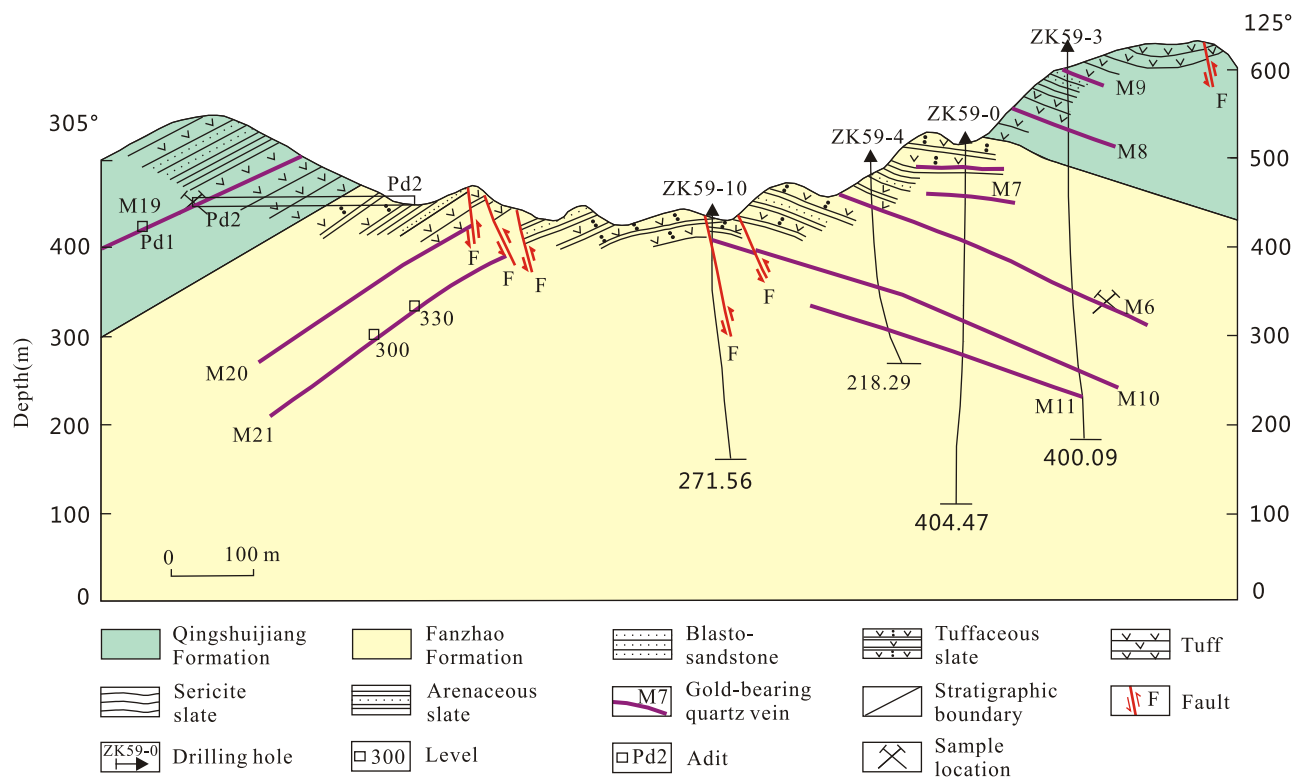


Figure 4. Geological map (A) and a cross-section (B) of the Pingqiu gold deposit (modified from Lu et al., 2006).



**Figure 5.** Geological profile of the No. 59 exploratory line of the Jinjing gold deposit, SE Guizhou.

15 g/t. The boundaries between the ore bodies and wall rocks are clear, with weak wall rock alterations, predominantly as silicification, sericitization, pyritization, and arsenopyritization.

The mineral parageneses are shown in Fig. 6. Arsenopyrite is widespread in both Pingqiu and Jinjing, and can generally be clarified into two stages. The earlier stage arsenopyrites primarily occur in altered slate that is neighbored with quartz veins (Fig. 7A–C), and they are disseminated and characterized by euhedral or subhedral, short-columnar, relatively coarse grains (0.5–4 mm) with a strong metal luster. Typically, these early-stage arsenopyrites occur alone, although they occasionally co-exist with pyrites. The later stage arsenopyrites occur in quartz veins that are cracked (Fig. 7D and E), with relatively fine grains (0.02–0.4 mm) occurring in aggregate and hosted in quartz veins with pyrite, sphalerite, galena, minor chalcopyrite and stibnite. Gold is primarily enriched in the arsenopyrite-quartz stage and polymetallic sulfide-quartz stage in sulfides, and occurs as native gold, typically in granular, arborescent, and irregular forms. In the present study, native gold was found in quartz from hand specimens (Fig. 7F) and in arsenopyrite under the microscope (Fig. 7C).

### 3. Sample preparation and analytical methods

The JJ-1 series arsenopyrite samples were collected from the altered slate of the No. 2 pit (Fig. 7A) of the Jinjing gold deposit, whereas the JJ-3 series samples were obtained from the quartz veins of the Yangmanchong ore block of the Jinjing gold deposit (Fig. 7B). The PQ-10 samples were collected from the altered slate of the Jinchangxi ore block, representing the Pingqiu gold deposit. All of the arsenopyrite samples were collected and separated carefully. Subsequently, fresh arsenopyrite samples were selected, crushed with a mortar, and sieved to 20–40 mesh, then handpicking was conducted under binocular microscope to achieve a purity of more than 99%.

Isotope measurements of Re and Os were conducted at the Re–Os Laboratory of the National Research Center of Geoanalysis (NRCC), Chinese Academy of Geological Sciences (CAGS), Beijing, using a high-resolution inductively coupled plasma mass spectrometer (HR-ICP-MS Element 2). The detailed analytical method has been summarized in Du et al. (2009). In brief, 1 g of the arsenopyrite sample was weighed accurately and loaded into a Carius tube and then mixed with the  $^{185}\text{Re}$  and  $^{190}\text{Os}$  spike, along with an appropriate amount ( $\sim 1$  mL) of ultrapure HCl loaded into the same tube. Then, in the following order, 2.5 mL 10 mol/L HCl, 8 mL 16 mol/L  $\text{HNO}_3$ , and 3 mL 30%  $\text{H}_2\text{O}_2$  were added to the tube. The tube was sealed and then heated in an oven at 200 °C for 24 h. After distillation of  $\text{OsO}_4$  at 105–110 °C, osmium was separated and trapped by Milli-Q water. During distillation, reverse aqua regia was used as the oxidizer. The straight adsorbent  $\text{OsO}_4$  liquid was used to determine Os isotope abundance. Rhenium was extracted from the residue with acetone in a 5 mol/L NaOH solution. Finally, the Re and Os isotopic compositions of arsenopyrite were measured by HR-ICP-MS. The intensity of the  $^{190}\text{Os}$  signal was monitored to correct the traces of Os in Re, and  $^{185}\text{Re}$  intensity was used to monitor traces of Re in Os.  $\text{H}_2\text{O}_2$  and 5% ammonia were used between samples to wash the Teflon injection tube to avoid cross-contamination between different samples.

The experimental procedure of noble gases can be described simply as follows. Weighed samples (approximately 0.3 g) for analyses were packed with aluminum foils and shifted to the crucible for gas extraction under high-vacuum conditions, heated to 130 °C after the pressure reached  $1 \times 10^{-5}$  Pa, and baked for more than 10 h at this temperature to remove the gas adsorbed by the sample surface (Ye et al., 2001). Then, the crucible was heated to 1600 °C, and the gases extracted from the samples were purified through activated charcoal traps at liquid nitrogen temperature to separate He and Ne from Ar + Kr + Xe for He and Ne analyses, and then for

Minerals/ stages	Barren quartz	Arsenopyrite (pyrite)-quartz	Polymetallic sulfide-quartz	Quartz-carbonate
Quartz	—————	—————	—————	—————
Chlorite	-----	-----	-----	-----
Sericite	-----	-----	-----	-----
Pyrite	-----	-----	-----	-----
Arsenopyrite	-----	-----	-----	-----
Native gold	-----	-----	-----	-----
Sphalerite	-----	-----	-----	-----
Galena	-----	-----	-----	-----
Chalcopyrite	-----	-----	-----	-----
Stibnite	-----	-----	-----	-----
Ferrodolomite	-----	-----	-----	-----
Calcite	-----	-----	-----	-----

**Figure 6.** Paragenetic sequence of main minerals in the Pingqiu and Jinjing gold deposits, SE Guizhou.

Ar + Kr + Xe analyses. “Standard–sample–standard” by using bracketing technique during the analysis process, and heat blanks were measured before each sample analysis. The noble gases were analyzed on a MM5400 mass spectrometer at the Lanzhou Center for Oil and Gas Resources, Institute of Geology and Geophysics, CAS, China, based on the following experimental conditions: emission current  $I_{t4} = 800 \mu\text{A}$ ,  $I_{t40} = 200 \mu\text{A}$ , and 9.000 kV as the high voltage. The maximum heat blanks of the MM5400 mass spectrometer are as follows:  $^4\text{He} = 1.10\text{E}-14 \text{ cm}^3\text{STP/g}$ ,  $^{20}\text{Ne} = 1.82\text{E}-14 \text{ cm}^3\text{STP/g}$ ,  $^{40}\text{Ar} = 6.21\text{E}-13 \text{ cm}^3\text{STP/g}$ ,  $^{84}\text{Kr} = 1.37\text{E}-16 \text{ cm}^3\text{STP/g}$ ,  $^{132}\text{Xe} = 5.65\text{E}-18 \text{ cm}^3\text{STP/g}$ . The standard (AIRLZ 2003) used was the air from Gaolan hilltop, Lanzhou City, China (Ye et al., 2001).

#### 4. Results

The Re and Os isotopic compositions of arsenopyrite samples from the Pingqiu (PQ) and Jinjing (JJ) gold deposits are shown in Table 1 and Fig. 8. The total procedure blanks, determination results, and recommendation values of monitoring samples (JCBY) are shown in Table 2. The confidence level is 95%. The reported uncertainties for Re and Os contents include those from sample weighing error and spikes, spike magnification, fractionation alignment errors inherent in measurements by mass spectrometer, and measurement errors of isotopic ratios. Stein et al. (2000) noted that blank correction appears to be particularly important for low-level sulfides that are highly radiogenic. The total blanks of Re and Os are low in this test (Table 2). In addition, the sample Re and Os contents are much higher than the blanks; therefore, blank corrections are not an issue. Moreover, the reference values (JCBY, Chen et al., 2015) determined in the present study are in agreement with the recommendations shown in Table 2. The repeat analysis generally agrees with the original analysis (PQ-6 (1) and (2), PQ-41 (1) and (2)). Suzuki et al. (2000) suggested that systematic replicate analyses are required to determine whether a Re–Os age has been affected by post-depositional alteration. Therefore, this method is probably the best way to assess whether the obtained results are precise and robust (Barra et al., 2003). The small differences in Re and Os characteristics between parallel samples may be due to the inhomogeneity of coarse-grained arsenopyrites. However, the analysis results for parallel samples are all consistent with the isochron, which in turn implies that the Re and Os isotopic system in arsenopyrite is closed; under these

closed conditions, the Re–Os isochron should not be impacted by such inhomogeneity.

The Re and Os concentrations reported in this paper are quite low, like those reported in Mikulski et al. (2005) and are generally one order of magnitude lower than those reported in Frei et al. (1998), Arne et al. (2001), and Morelli et al. (2005). However, the low Re and Os samples can also yield precise results (Hnatyshin et al., 2015). Therefore, the relatively large uncertainty in this report was assessed to be a combination of the very low Re and Os concentrations and the ICP-MS technique was used (Barra et al., 2003; Mikulski et al., 2005).

Two sets of  $^{187}\text{Re}/^{188}\text{Os}$ – $^{187}\text{Os}/^{188}\text{Os}$  isochron ages were calculated using Isoplot V. 3.23 (Ludwig, 2005). An age of  $400 \pm 24 \text{ Ma}$ ,  $\text{MSWD} = 0.96$  and an initial  $^{187}\text{Os}/^{188}\text{Os}$  ( $\text{Os}_i$ ) =  $1.24 \pm 0.57$  were obtained for the arsenopyrite from Pingqiu, respectively, whereas an age of  $400 \pm 11 \text{ Ma}$  with  $\text{MSWD} = 0.34$ , and  $\text{Os}_i = 1.55 \pm 0.14$  were obtained for the Jinjing gold deposit. The error correlation ( $\rho$ ) values for all samples range from 0.254 to 0.952. Although certain analytical errors (11–24 Ma) exist, both isochronal ages coincide with each other very well. Based on the above analysis of the experimental process and result (e.g., Repeat analysis, and JCBY monitoring), it is suggested that the analytical results in this test are reliable. Moreover, the dating samples of gold-bearing arsenopyrites were all chosen from the arsenopyrite (pyrite)–quartz stage, and they are euhedral and unaltered by means of microscopic analysis. As a result, the isochron ages in this study is considered to be reliable and reflect the ore formation time for the Pingqiu and Jinjing gold deposits. In addition, the samples had similar  $\text{Os}_i$  ratios, which indicates the same origin.

The results of the He and Ar isotope analyses of fluid inclusions, together with U and Th concentrations, in the arsenopyrites from the two deposits are listed in Table 3 and shown in Figs. 9 and 10. It is clear from Table 3 that the Pingqiu arsenopyrite samples exhibit higher  $^4\text{He}$ ,  $^{40}\text{Ar}$ , Th, and U concentrations than the Jinjing samples. All of the arsenopyrite samples show positive correlations between Th and  $^4\text{He}$  (Fig. 11A) and between U and  $^4\text{He}$  (Fig. 11B).

#### 5. Discussion

##### 5.1. Metallogenic epoch

The two Re–Os isochron ages obtained from arsenopyrite in the Pingqiu and Jinjing gold deposits are completely consistent (400 Ma). Focusing on the perspective of the whole Jiangnan Orogenic Belt, this age corresponds to the Caledonian (Late Silurian), is consistent with a  $402 \pm 6 \text{ Ma}$  Sm–Nd isochron age for scheelite, and overlaps with four plateau ages of  $416.2 \pm 0.8 \text{ Ma}$ ,  $423.2 \pm 6 \text{ Ma}$ ,  $397.4 \pm 0.4 \text{ Ma}$  and  $422.2 \pm 0.2 \text{ Ma}$ , dated by the  $^{40}\text{Ar}$ – $^{39}\text{Ar}$  method for quartz from Au-bearing quartz veins from the Woxi and Banxi gold deposits in western Hunan (Peng et al., 2003). Within the uncertainty, this age is in good agreement with the quartz fluid inclusion Rb–Sr isotope ages of  $406 \pm 25 \text{ Ma}$ ,  $412 \pm 33 \text{ Ma}$  and  $435 \pm 9 \text{ Ma}$  from the Jinshang gold deposit in northeast Zhejiang (Wang et al., 1999) and from the Xiaojia and Pingcha gold deposits in western Hunan (Peng and Dai, 1998), respectively. In addition, this age is also coincident with the feldspar K–Ar isotope ages of 404–412 Ma from the Mobin and Liulinchai gold deposits in western Hunan (Wang et al., 1999).

The Caledonian movement had a significant impact on the regional sedimentary framework, deformation, and metamorphism (Lu et al., 2005). A series of geological observations are indicative of the region’s Caledonian tectonic activity, including the following: an unconformity between the Middle–Late Devonian and Pre-Devonian sequences; the absence of Late Silurian sediments; and the inconsistency of folding styles between the Pre-Devonian and

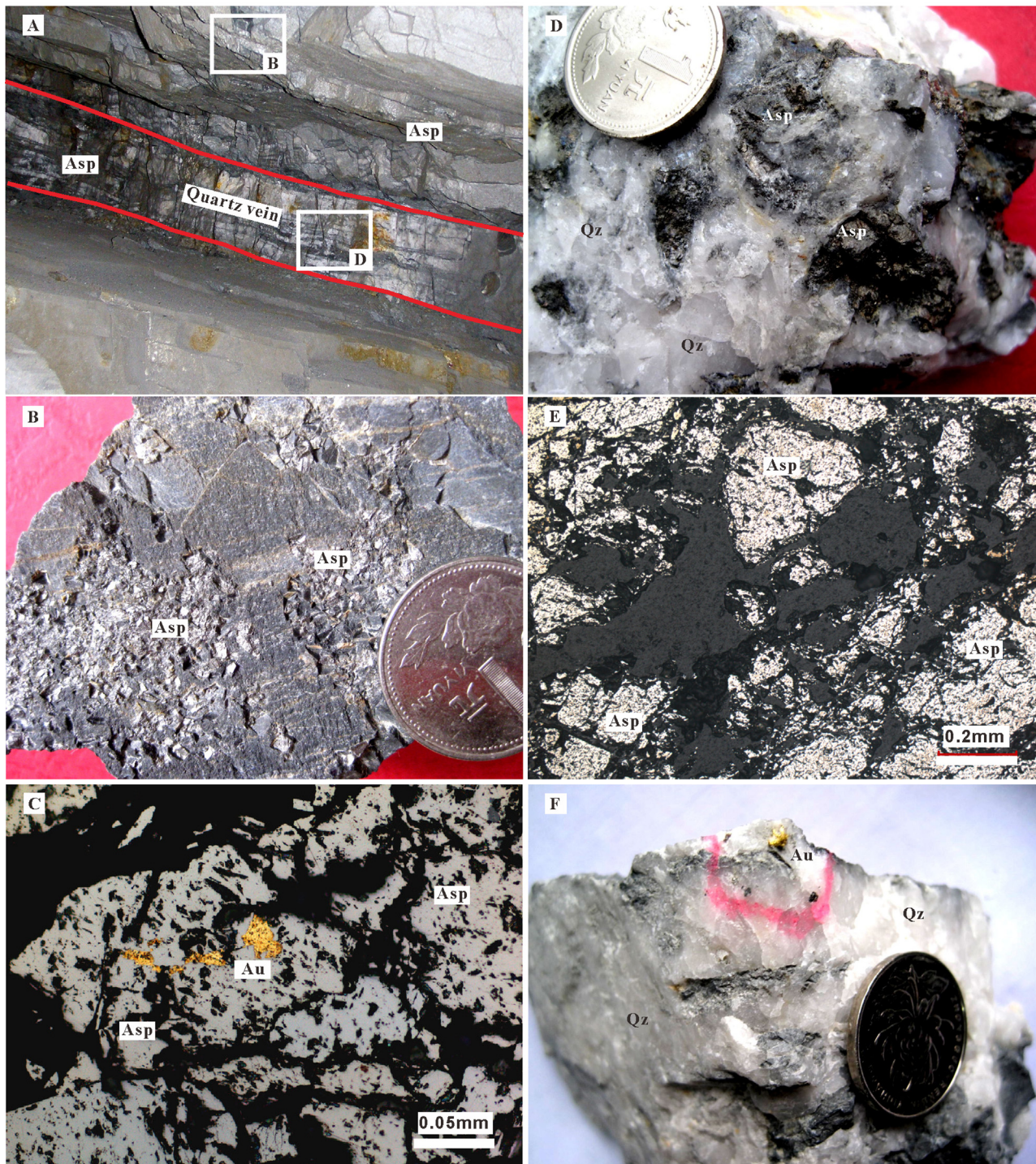


**Figure 7.** Photographs of field, hand specimen and microphotographs of thin section from the Jinjing gold deposit, SE Guizhou, China. (A) Field photograph of arsenopyrites occur in altered slate and quartz veins; (B) euhedral arsenopyrites of arsenopyrite (pyrite)-quartz stage, occur in altered slate; (C) native gold occurs in arsenopyrites; (D) arsenopyrites of polymetallic sulfide-quartz stage, occur in quartz veins; (E) microphotograph of arsenopyrites (polymetallic sulfide-quartz stage) with cataclastic texture; (F) native gold occurs in quartz veins. Abbreviations: Asp-Arsenopyrite, Qz-quartz, Au-gold.

Late Paleozoic strata and the voluminous Silurian granitic intrusions (JXBGM, 1984; Wang et al., 2007). In particular, the EW-trending fault in the region, including the Gaoniang and Qimeng shear zones, was formed during this period (Lu et al., 2005, 2006). The illite K–Ar geochronology of the Banxi Group slate suggests that the Caledonian tectonothermal event occurred as early as  $418.8 \pm 6.7$  Ma, and the cooling ages dated at 419–389 Ma by illite K–Ar geochronology demonstrate the unroofing and uplifting time

of the Caledonian orogeny (Hu et al., 2010). The uplift of the Xuefeng block and the formation of its western boundary (the Zhangjiajie–Huayuan–Kaili fault zone) were a direct result of Caledonian tectonic activity in South China (Hu et al., 2010). Based on zircon U–Pb data, and in combination with other geochronological data and geological observations throughout the South China Block, Wang et al. (2007) proposed that the Caledonian tectonothermal event around the Silurian (450–400 Ma) might have been the



**Table 1**

Re–Os isotopic data for arsenopyrites from the Pingqiu and Jinjing gold deposits, SE Guizhou, China.

Sample No.	Sample weight (g)	Re (ng/g)		Common Os (ng/g)		$^{187}\text{Os}$ (ng/g)		$^{187}\text{Re}/^{188}\text{Os}$		$^{187}\text{Os}/^{188}\text{Os}$		rho
		Re	2 $\sigma$	Os	2 $\sigma$	$^{187}\text{Os}$	2 $\sigma$	Ratio	2 $\sigma$	Ratio	2 $\sigma$	
PQ-6 (1)	1.000	0.2947	0.0064	0.0016	0.0001	0.0015	0.0000	905.7	41.0	7.540	0.328	0.800
PQ-6 (2)	1.001	0.2225	0.0020	0.0017	0.0001	0.0012	0.0000	633.6	47.9	5.387	0.422	0.952
PQ-18	1.001	0.5905	0.0049	0.0016	0.0000	0.0027	0.0001	1751	36	12.88	0.34	0.639
PQ-28	1.000	2.5713	0.0190	0.0053	0.0001	0.0118	0.0002	2355	65	17.20	0.54	0.811
PQ-41 (1)	1.000	0.3863	0.0030	0.0010	0.0001	0.0018	0.0000	1843	121	13.93	0.97	0.930
PQ-41 (2)	1.101	0.3384	0.0033	0.0012	0.0000	0.0016	0.0000	1416	46	10.42	0.34	0.902
JJ-1-1	1.099	0.8020	0.0066	0.0011	0.0000	0.0036	0.0000	3451	83	24.44	0.62	0.845
JJ-1-2	1.102	0.3038	0.0059	0.0015	0.0000	0.0016	0.0000	972.5	20.3	8.102	0.089	0.254
JJ-1-7	1.101	0.6096	0.0086	0.0015	0.0000	0.0028	0.0000	1991	61	14.76	0.41	0.879
JJ-1-9	1.102	0.6477	0.0080	0.0012	0.0000	0.0030	0.0000	2512	85	18.56	0.58	0.937
JJ-1-13	1.102	0.5697	0.0046	0.0048	0.0000	0.0034	0.0000	575.9	7.5	5.389	0.052	0.825
JJ-1-18	1.100	0.5419	0.0065	0.0040	0.0000	0.0031	0.0000	651.7	10.8	5.940	0.080	0.578

Note:  $^{187}\text{Re}$  decay constant =  $1.666 \times 10^{-11} \text{ yr}^{-1}$  (Smoliar et al., 1996); the Re,  $^{187}\text{Os}$ , and common Os concentration data are blank corrected;  $^{187}\text{Os}$  values represent total  $^{187}\text{Os}$ ; PQ-6(1) and (2), PQ-41(1) and (2) belong to the same samples, and they were analyzed for twice, separately; PQ = Pingqiu, JJ = Jinjing.

result of an intracontinental collision between the Yangtze and Cathaysian blocks. Accordingly, we suggest that the Caledonian was a significant gold mineralization period in South China, especially in the Jiangnan Orogenic Belt. The intracontinental collision between the Yangtze and Cathaysian blocks likely provided the geological background tectonization for the formation of gold (Goldfarb et al., 2014).

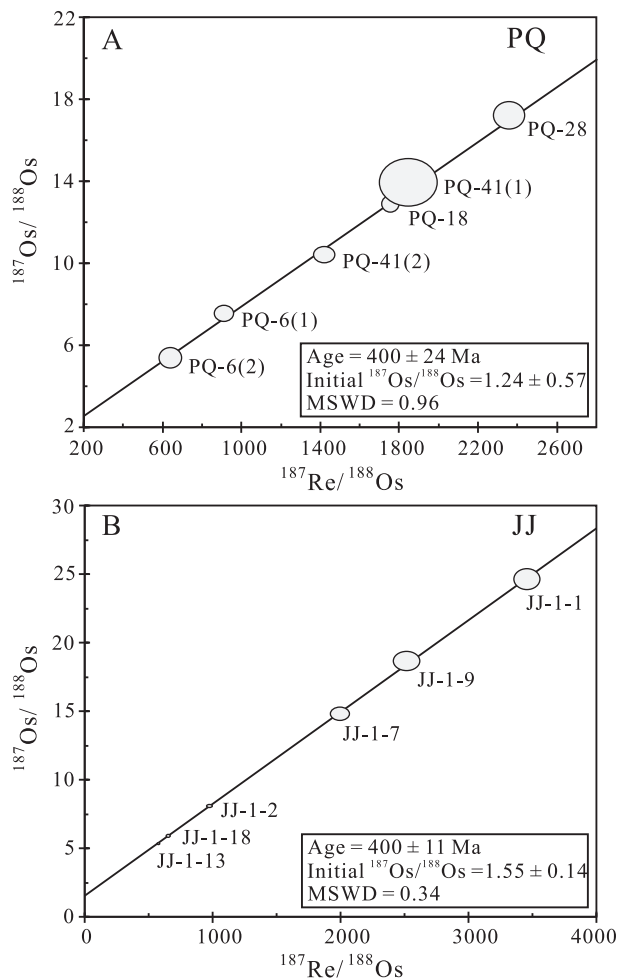


**Figure 8.** Re–Os isochron diagrams of arsenopyrite from the Pingqiu (A) and Jinjing (B) gold deposits, SE Guizhou, China. The circles with different sizes represent different analytical uncertainties, the bigger in size, the larger in uncertainty within individual sample.

Previous studies have verified that the Indosinian–Yanshanian movement (240–140 Ma) had a great influence on the Xuefeng area, particularly the south margin of the Xuefeng gold district, as evidenced by the Indosinian and Yanshanian igneous rocks in the Zhonghuashan, Canshuipu, and Yangcaichong areas and the granite–porphyry dykes in the Fuzhuxi and Banxi regions (Liu, 1993). Zhao et al. (2005) reported the whole rock K–Ar geochronology age of Banxi granite–porphyry to be  $194.16 \pm 4.05$  Ma and  $202.03 \pm 4.40$  Ma. Peng and Frei (2004), using an  $^{87}\text{Sr}/^{86}\text{Sr}$ –1/Sr mixing diagram of sphalerite and stibnite from Woxi, reported an age of  $199 \pm 8$  Ma; simultaneously, they suggested that the formation of the gold deposits may be related to the emplacement of Indosinian–Yanshanian granitoids. Through sericite Ar–Ar geochronology, an age of 180–175 Ma ( $175.4 \pm 1.2$  Ma,  $175.3 \pm 1.1$  Ma,  $178.2 \pm 1.4$  Ma, and  $179.6 \pm 2.9$  Ma) was obtained from the Yinshan gold deposit of the northeast Jiangnan Orogenic Belt (Li et al., 2006). Data based on sericite, biotite, and muscovite  $^{40}\text{Ar}/^{39}\text{Ar}$  geochronology and other geological observations (Wang et al., 2005) have also revealed a phase of the major deformation event in the Xuefengshan tectonic belt to be constrained to the middle Triassic to early Jurassic ( $194.7 \pm 0.3$  Ma,  $216.9 \pm 0.3$  Ma,  $207.2 \pm 0.2$  Ma,  $215.3 \pm 0.8$  Ma, and  $213.5 \pm 0.2$  Ma). Consequently, as Goldfarb et al. (2014) suggested, for most of the Jiangnan Orogenic Belt, the time of gold formation was Caledonian; however, the middle to late Mesozoic age cannot be ruled out for at least some of the ores.

## 5.2. Constraints on metals and fluids sources

### 5.2.1. Initial Os isotope compositions

Many previous studies (e.g., Arne et al., 2001; Barra et al., 2003; Morelli et al., 2005, 2007) have applied the Re–Os isotopic system to constrain the origin of ore metals owing to the remarkable fractionation of Re and Os between the mantle and crust. Re is a

**Table 2**

The total procedure blanks, determination of monitoring sample (reference material JCBY) and its recommendation data.

Blank No.	Re (ng)		Common Os (ng)		$^{187}\text{Os}$ (ng)	
	Re	2 $\sigma$	Os	2 $\sigma$	$^{187}\text{Os}$	2 $\sigma$
BK-01	0.0055	0.0003	0.0001	0.0001	0.0001	–
BK-02	0.0031	0.0001	0.0003	0.0001	0.0003	0.0002
Sample No.	Re (ng/g)		Total Os (ng/Sg)		$^{187}\text{Os}/^{188}\text{Os}$	
	Re	2 $\sigma$	Os	2 $\sigma$	Ratio	2 $\sigma$
JCBY	39.14	0.40	16.16	0.13	0.3345	0.0026
Recommendation	38.61	0.54	16.23	0.17	0.3363	0.0029

**Table 3**  
He and Ar isotopic compositions of fluid inclusion and Th and U contents of arsenopyrites.

Sample No.	Weight (g)	$^4\text{He}$ ( $\text{cm}^3\text{STP/g}$ )	$^{40}\text{Ar}$ ( $\text{cm}^3\text{STP/g}$ )	$^3\text{He}/^4\text{He}$ (Ra)	$^{40}\text{Ar}^*/^4\text{He}$ (E-2)	$^3\text{He}/^{36}\text{Ar}$ (E-4)	$^{40}\text{Ar}/^{36}\text{Ar}$	Th (ppm)	U (ppm)
JJ-3-1	0.301	1.22E-06	2.15E-07	6.84E-03	13.41	0.66	1225.6	<0.05	<0.05
JJ-3-2	0.301	3.07E-06	2.63E-07	5.87E-03	7.89	3.57	3724.6	<0.05	<0.05
JJ-3-5	0.298	1.83E-06	2.33E-07	1.88E-02	9.68	2.54	1231.9	<0.05	<0.05
JJ-3-9	0.299	3.00E-06	1.53E-07	1.27E-02	3.14	2.68	769.6	0.14	0.05
JJ-3-10	0.300	1.19E-06	2.05E-07	2.54E-02	14.09	3.35	1624.9	0.19	<0.05
PQ-6	0.299	2.41E-06	2.79E-07	8.45E-03	6.17	0.65	633.2	0.05	<0.05
PQ-17	0.399	6.66E-06	4.49E-07	2.66E-03	4.59	0.51	925.7	0.17	0.08
PQ-18	0.299	1.58E-05	5.07E-07	1.90E-02	3.06	54.53	6582.0	0.50	0.14
PQ-28	0.400	6.06E-05	4.39E-07	5.33E-04	0.64	2.50	2429.5	2.4	0.63
PQ-32	0.401	1.20E-05	2.44E-06	1.48E-02	15.39	1.26	1228.6	0.09	<0.05

moderately incompatible element and more likely to separate into the magma during mantle melting; conversely, Os is a highly compatible element and tends to be retained in the mantle. Furthermore, both Au and Os are precious metals and share certain geochemical properties, for example, they are both soluble as a variety of molecular species in aqueous and  $\text{CO}_2$ -rich fluids; thus, Os isotopic analysis holds some promise as an isotopic tracer for solution-mobilized Au mineralization (Shirey and Walker, 1998).

The initial  $^{187}\text{Os}/^{188}\text{Os}$  ratios ( $\text{Os}_i$ ) of the arsenopyrite from Pingqiu and Jinjing are  $1.24 \pm 0.57$  and  $1.55 \pm 0.14$ , respectively. Both  $\text{Os}_i$  ratios are remarkably above their typical value in the mantle (0.12–0.13; Shirey and Walker, 1998). This range (1.24–1.55) is completely overlapping with typical crustal ( $\sim 1.0$ –1.5)  $^{187}\text{Os}/^{188}\text{Os}$  ratios (Arne et al., 2001; Cardon et al., 2008), indicating a significant crustal component for the source of Os, and by inference, Au in arsenopyrite. In addition, such Os characteristics are the same as most of the orogenic gold deposits of Phanerozoic age worldwide, such as the 408 Ma Owens gold occurrence in the southwestern Meguma terrane, Canada, with arsenopyrite  $\text{Os}_i$  values of  $0.83 \pm 0.16$  (Morelli et al., 2005), and the 438 Ma Bendigo deposit of central Victoria, Australia, for pyrite  $\text{Os}_i$  values of  $1.04 \pm 0.16$  (Arne et al., 2001). In addition, these arsenopyrites from southeastern Guizhou exhibit a similar REE pattern to the wall rocks of the Xiajiang Group, indicating that the ore materials were likely derived from wall rocks (Wang, 2012). This interpretation is also supported by other studies based on sulfides and wall rocks S–Pb isotopes, REE and trace element study of wall rocks and ores. It was found that the S–Pb isotopes in sulfides are in good

agreement with those of wall rocks, and the REE and trace element characteristics in ores have been inherited from the wall rocks. Therefore, Peng et al. (1999) suggested that the ore-forming materials of the gold deposits in southwestern Hunan (neighbored southeastern Guizhou) mainly came from the wall rocks of Proterozoic strata. Ma et al. (2002) systematically studied trace element geochemical characteristics of Au deposits in central Hunan and discussed the ore source of ore-forming metals. The ore-forming metal (Au) is higher in Proterozoic basement clastics (3.1–7.2 ppm) relative to Paleozoic strata (0.4–1.5 ppm), and the leaching experiment shows that the leaching ratio of Au in clastics may reach 19%–86%; meanwhile, Au abnormality clearly exists around ore bodies of Au deposits that occur in clastics, and the REE contents and distribution patterns of ores are similar to those of basement clastics. Therefore, they also suggested that the basement clastics are the ore source of Au deposits in the central Hunan basin. Based on the Nd–Sr–Pb isotope study on scheelite, inclusion fluids and residues of gangue quartz, and sulfides from the gold deposit at Woxi and Liaojiaping in the Xuefeng region, western Hunan, Peng and Frei (2004) indicated that the  $\epsilon_{\text{Nd}}$  values are around  $-10$  for the Liaojiaping and compare well with the range of  $-5$  to  $-10$  defined by the granitoids, whereas they are around  $-27$  for scheelite from Woxi. Sr isotopes of scheelite shows that  $^{87}\text{Sr}/^{86}\text{Sr}$  ratios of  $\sim 0.721$  for Liaojiaping scheelite agree with values ranging between 0.718 and 0.726 for granitoids, whereas the ratio for scheelite from Woxi is much higher at  $\sim 0.745$ , as is the  $^{87}\text{Sr}/^{86}\text{Sr}$  ratio range of 0.743–0.749 for Precambrian host slates. In addition, Pb isotopes reveal upper crustal signatures and are compatible with Pb isotope signatures of the predominant Precambrian slates in the

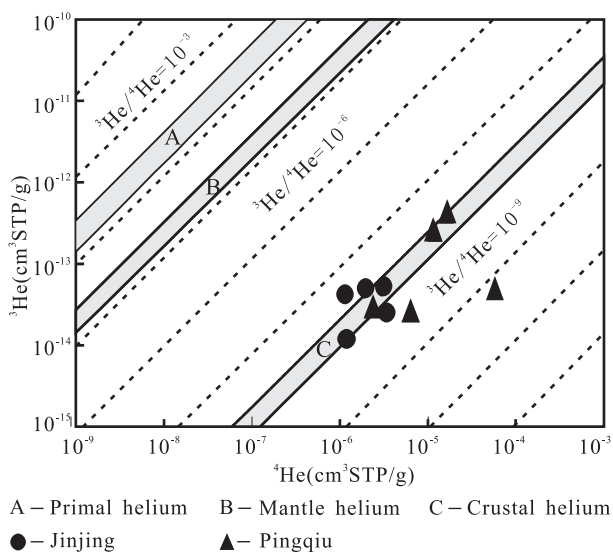


**Figure 9.** Helium isotopes of inclusion-trapped fluids from arsenopyrite in the Pingqiu and Jinjing gold deposits, SE Guizhou, China.

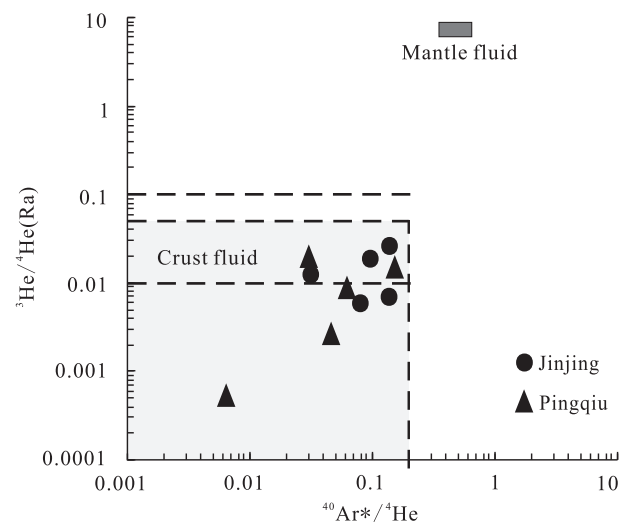


**Figure 10.**  $^{40}\text{Ar}^*/^4\text{He}$  vs.  $^3\text{He}/^4\text{He}$  plot of inclusion-trapped fluids from arsenopyrites in the Pingqiu and Jinjing gold deposits, SE Guizhou, China.

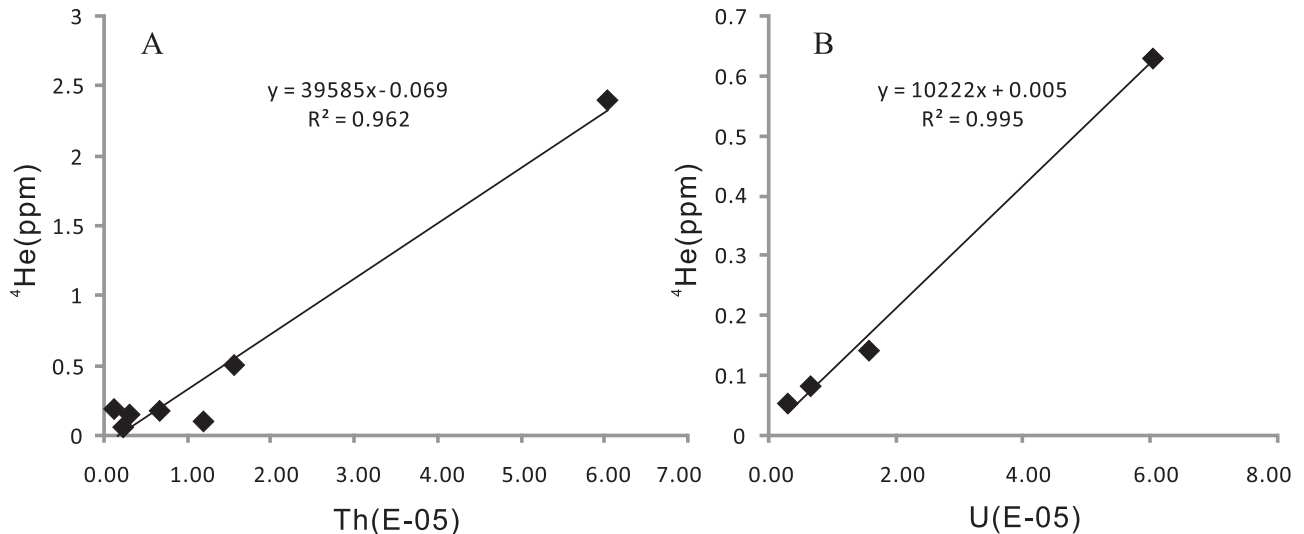


**Figure 11.** (A) Th versus  $^4\text{He}$  diagram, and (B) U versus  $^4\text{He}$  diagram of inclusion-trapped fluids from arsenopyrites in the Pingqiu and Jinjing gold deposits, SE Guizhou, China.

Woxi area, whereas the Pb isotopic characteristics reflect less radiogenic compositions compatible with fluids originating from the widespread Indosinian-Yanshanian granitoids emplaced within the Xuefeng region. The above Nd–Sr–Pb isotopic characteristics imply that the Proterozoic basement clastics are ore sources of the Woxi gold deposit, and the Indosinian-Yanshanian granitoids are possible candidates for Liaojiaping. Considering that the Liaojiaping W–Sb–Au occurrence is developed within Paleozoic black shale and is spatially and temporally related to Indosinian-Yanshanian granite porphyry dykes (Peng and Frei, 2004), whereas Pingqiu and Jinjing are the same as Woxi and are developed within Proterozoic strata, and no magmatic rocks are outcropped in these regions, therefore, it is reasonable that the primary sources of the ore-forming elements of the Pingqiu and Jinjing gold deposits are the ore-bearing rocks of the Proterozoic Xiajiang Group.

### 5.2.2. He–Ar isotopes

Since the 1990s, He and Ar isotopes have been widely applied to trace sources of ore-bearing fluids (e.g., Stuart et al., 1994, 1995; Hu et al., 1999, 2004; 2009; Wu et al., 2011). The He isotope tracing method is particularly useful in differentiating mantle and crustal fluid sources owing to the three orders of magnitude difference in He isotope ratios between the mantle and crustal reservoirs. The  $^3\text{He}/^4\text{He}$  ratio in the mantle is approximately 6–9 Ra, whereas the  $^3\text{He}/^4\text{He}$  ratio in the crust is approximately 0.01 Ra (Stuart et al., 1995). Consequently, the  $^3\text{He}/^4\text{He}$  ratio of a crustal ore-bearing fluid undergoes an obvious change when the mantle He input increases, even for only small additions of mantle fluid. Generally, there are four sources of He in crustal fluids: mantle He, crustal He, atmospheric He, and cosmogenic He (Ballentine and Burnard, 2002). The  $^3\text{He}/^36\text{Ar}$  ratios of all samples studied here are clearly higher than the air value ( $2.4 \times 10^{-7}$ ), and the arsenopyrite samples were all collected from underground, where atmospheric and cosmogenic He contamination is negligible or can simply be excluded (Simmons et al., 1987; Stuart et al., 1995). Therefore, for the gold ore-bearing fluid in Southeast Guizhou, the major possible sources are the crust and mantle.

In contrast to previous results obtained from Hu et al. (2004, 2009), the concentrations of both  $^4\text{He}$  and Ar are higher in the present study. Some of the samples yielded  $^3\text{He}/^4\text{He}$  ratios significantly higher than typical crustal values. This may have been caused by in situ generation of  $^4\text{He}$  due to the radioactive decay of U and Th, which may be present as dissolved constituents in inclusion

fluids or as impurities in host minerals (Simmons et al., 1987). The positive correlations between Th and  $^4\text{He}$  (Fig. 11A) and between U and  $^4\text{He}$  (Fig. 11B) indicate that the arsenopyrite contains relatively high concentrations of Th, U, and  $^4\text{He}$ , particularly compared to  $^3\text{He}/^4\text{He}$  ratios. In the most extreme case, sample PQ-28 revealed the highest concentrations of Th (2.4 ppm), U (0.63 ppm), and  $^4\text{He}$  ( $6.06 \times 10^{-5}$ ); these concentrations are 5–50 times higher than those of other samples and were associated with the lowest measured  $^3\text{He}/^4\text{He}$  ratio ( $5.33 \times 10^{-4}$ ) and  $^{40}\text{Ar}^*/^4\text{He}$  ratio ( $0.64 \times 10^{-2}$ ).

By calculation, if an arsenopyrite sample contains U and Th (1 ppm for each), under 400 Ma years of radioactive decay,  $0.65 \times 10^{-6}$  and  $0.12 \times 10^{-6}$   $\text{cm}^3(\text{STP})/\text{g}$   $^4\text{He}$  will be generated, respectively. Considering the lowest content of  $^4\text{He}$  in all of the samples is  $1.19 \times 10^{-6}$   $\text{cm}^3(\text{STP})/\text{g}$ , we suggest that at the condition of U and Th (<0.1 ppm for each) ( $\sim 400$  Ma), especially for U, the radioactive decay product of  $^4\text{He}$  would be lower than 10%, and the  $^4\text{He}$  analytical precision can be guaranteed. Therefore, in our present study, except samples PQ-18 and PQ-28, there is limited impact to  $^4\text{He}$  by U and Th radioactive decay for all other samples. Figs. 9 and 10 show that most samples fall within the crustal area, with typical  $^3\text{He}/^4\text{He}$  ratios of approximately 0.01 Ra (Stuart et al., 1995) or < 0.1 Ra (Simmons et al., 1987),  $^{40}\text{Ar}^*/^4\text{He}$  ratios of 0.2 (Stuart et al., 1995), and  $^{40}\text{Ar}^*/^{36}\text{Ar}$  ratios of  $\geq 1000$  (Drescher et al., 1998). The He–Ar inference of crustal origin is in good agreement with the  $\text{Os}_i$  evidence discussed previously. In addition, such a conclusion is also supported by Zhu and Peng (2015) on the basis of a pyrite and stibnite He–Ar isotope study for the Woxi gold deposit in western Hunan, China.

In addition, a series of petrographic, micro-thermometric, and laser Raman spectroscopic studies have been conducted on fluid inclusions (FI) in ore-bearing quartz from the Pingqiu and Jinjing gold deposits (Wang, 2012). For the Pingqiu deposit, the homogenization temperatures and salinity levels range from 230 °C to 350 °C and 1.81 wt.% to 5.51 wt.% NaCl equiv., respectively; for the Jinjing deposit, the homogenization temperatures and salinity levels range from 200 °C to 310 °C and 1.22 wt.% to 3.52 wt.% NaCl equiv., respectively. These results demonstrate that the ore-forming fluids for both ore deposits are characterized by a medium-low temperature and low salinity. Based on our studies on the hydrogen and oxygen isotopes of quartz (Wang, 2012), the results show that the ore-bearing fluids of the Pingqiu gold deposit ( $\delta\text{D} = -46\text{‰}$  to  $-67\text{‰}$ ,  $\delta^{18}\text{O}_{\text{water}} = 9.3\text{‰}$ – $11\text{‰}$ ) and, Jinjing

gold deposit ( $\delta D = -50\text{‰}$  to  $-57\text{‰}$ ,  $\delta^{18}\text{O}_{\text{water}} = 8.2\text{‰}$ – $9.1\text{‰}$ ) correspond to metamorphic fluid, though magmatic sources cannot yet be ruled out. Apart from the above characteristics, the ore-forming fluids of the Pingqiu and Jinjing deposits are also characterized as being  $\text{CO}_2$ -rich and  $\text{N}_2$ -bearing (Wang, 2012). These characteristics are in good agreement with the characteristics of the orogenic Woxi gold deposit, with low-to-moderate temperature (109–354 °C), low salinity (<7 wt.% NaCl equiv.), and  $\text{CO}_2$ -rich and  $\text{N}_2$ -bearing aqueous fluids, and those gold deposits are widespread in the Xuefeng region, which were summarized by Zhu and Pen (2015). In addition, such geological and geochemical features in Pingqiu and Jinjing are compatible with orogenic gold deposits (Groves et al., 1998; Goldfarb et al., 2001, 2014; Zhu and Pen, 2015).

Summing up the above discussion and previous studies, a conceptual genetic model of the gold deposits in Southeastern Guizhou is proposed as follows. (1) During the Proterozoic, the Xiajiang Group volcano-sedimentation laid the basis for the source rocks of the gold deposit. (2) In the Caledonian orogeny, folds (anticlines and synclines) and shear zones developed with low-grade regional metamorphism, and the gold-bearing metamorphic fluids formed simultaneously. Then, the fluids were cycled and transported under the forces of tectonic activity. Finally, gold was precipitated, and ore bodies formed at suitable locations under the appropriate physicochemical conditions.

## 6. Conclusions

- (1) This study reports two Caledonian mineralization ages of  $400 \pm 24$  Ma (MSWD = 0.96) and  $400 \pm 11$  Ma (MSWD = 0.34) using the Re–Os isotope system to analyze auriferous arsenopyrites from the Pingqiu and Jinjing orogenic gold deposits. These ages are in agreement with regional geochronological data and correspond to the regional Caledonian orogeny. It is confirmed that the Caledonian is an important gold mineralization period in Southeast Guizhou, and likely throughout the Jiangnan Orogenic Belt.
- (2) The ore-forming metal elements of the Pingqiu and Jinjing gold deposits may have been derived primarily from the ore-bearing Xiajiang Group, and the fluids may have been sourced from the metamorphic water, though magmatic water cannot be ruled out, based on the initial  $^{187}\text{Os}/^{188}\text{Os}$  ratios and He–Ar isotopic values.
- (3) It should be noted that the amount of in situ radiogenic  $^4\text{He}$  generated should not be ignored in noble gas studies, even when Th and U are present at levels of only a few ppm in host minerals.

## Acknowledgement

We are grateful to Prof. Xianren Ye (Lanzhou Center for Oil and Gas Resources, Institute of Geology and Geophysics, CAS, China) for He–Ar analyses. Special thanks are also due to Profs. Yuzhuo Qiu and Zhuwei Jiang for fruitful discussion and improvement of the manuscript. This research is jointly supported by the National Natural Science Foundation of China (Grant Nos. 41303038, 41772070), Open Fund of State Key Laboratory of Ore Deposit Geochemistry (201502), and the National Basic Research Program of China (2014CB440904). The constructive comments from Prof. Shengrong Li, Drs. Yang Li and Xiaohua Deng, an anonymous reviewer and editorial handling by Dr. Stijn Glorie and Dr. Lili Wang are highly appreciated.

## References

- Arne, D.C., Bierlein, F.P., Morgan, J.W., Stein, H.J., 2001. Re–Os dating of sulfides associated with gold mineralization in central Victoria, Australia. *Economic Geology* 96, 1455–1459.
- Ballentine, C.J., Burnard, P.G., 2002. Production, release and transport of noble gases in the continental crust. *Reviews in Mineralogy and Geochemistry* 47, 481–538.
- Bao, Z.X., 1991. A discussion on gold potential of pyrite and arsenopyrite in gold-bearing deposit, Hunan province. *Mineral Resources and Geology* 24, 368–374 (in Chinese with English abstract).
- Barra, F., Ruiz, J., Mathur, R., Tittle, S., 2003. A Re–Os study of sulfide minerals from the Bagdad porphyry Cu–Mo deposit, northern Arizona, USA. *Mineralium Deposita* 38, 585–596.
- Cardon, O., Reisberg, L., Sylvie, A., Andre-Mayer, A.S., Leroy, J., Milu, V., Zimmermann, C., 2008. Re–Os systematics of pyrite from the Bolcana porphyry copper deposit, Apuseni Mountains, Romania. *Economic Geology* 103, 1695–1702.
- Chen, M.H., Mao, J.W., Li, C., Zhang, Z.Q., Dang, Y., 2015. Re–Os isochron ages for arsenopyrite from Carlin-like gold deposits in the Yunnan–Guizhou–Guangxi “golden triangle”, southwestern China. *Ore Geology Reviews* 64, 316–327.
- Deng, Q., Wang, J., Wang, Z.J., Cui, X.Z., Shi, M.F., Du, Q.D., Ma, L., Liao, S.Y., Ren, G.M., 2016. Middle neoproterozoic magmatic activities and their constraints on tectonic evolution of the Jiangnan orogen. *Geotectonica et Metallogenia* 40, 753–771.
- Deng, X.H., Chen, Y.J., Santosh, M., Zhao, G.C., Yao, J.M., 2013. Metallogeny during continental outgrowth in the Columbia supercontinent: isotopic characterization of the Zhaiwa Mo–Cu system in the north China Craton. *Ore Geology Reviews* 51, 43–56.
- Deng, X.H., Wang, J.B., Pirajno, F., Wang, Y.W., Li, Y.C., Li, C., Zhou, L.M., Chen, Y.J., 2016a. Re–Os dating of chalcopyrite from selected mineral deposits in the Kalatag district in the eastern Tianshan Orogen, China. *Ore Geology Reviews* 77, 72–81.
- Deng, X.H., Chen, Y.J., Santosh, M., Yao, J.M., Sun, Y.L., 2016b. Re–Os and Sr–Nd–Pb isotope constraints on source of fluids in the Zhifang Mo deposit, Qinling Orogen, China. *Gondwana Research* 30, 132–143.
- Drescher, J., Kirsten, T., Schäfer, K., 1998. The rare gas inventory of the continental crust, recovered by the KTB continental deep drilling project. *Earth and Planetary Science Letters* 154, 247–263.
- Du, A.D., Qu, W.J., Li, C., Yang, G., 2009. A review on the development of Re–Os isotopic dating methods and techniques. *Rock and Mineral Analysis* 28, 288–304 (in Chinese with English abstract).
- Feng, C.Y., Qu, W.J., Zhang, D.Q., Dang, X.Y., Du, A.D., Li, D.X., She, H.Q., 2009. Re–Os dating of pyrite from the Tuolugou stratabound Co (Au) deposit, eastern Kunlun Orogenic Belt, northwestern China. *Ore Geology Reviews* 36, 213–220.
- Frei, R., Nägler, T.F., Schönberg, R., Kramers, J.D., 1998. Re–Os, Sm–Nd, U–Pb, and stepwise lead leaching isotope systematics in shear-zone hosted gold mineralization: genetic tracing and age constraints of crustal hydrothermal activity. *Geochimica et Cosmochimica Acta* 62, 1925–1936.
- Freydier, C., Ruiz, J., Chesley, J., McCandless, T., Munizaga, F., 1997. Re–Os isotope systematics of sulfides from felsic igneous rocks: application to base metal porphyry mineralization in Chile. *Geology* 25, 775–778.
- Goldfarb, R.J., Groves, D.I., Gardoll, S., 2001. Orogenic gold and geologic time: a global synthesis. *Ore Geology Reviews* 18, 1–75.
- Goldfarb, R.J., Taylor, R.D., Collins, G.S., Goryachev, N.A., Orlandini, O.F., 2014. Phanerozoic continental growth and gold metallogeny of Asia. *Gondwana Research* 25, 48–102.
- Groves, D.I., Goldfarb, R.J., Gebre-Mariam, M., Hagemann, S.G., Robert, F., 1998. Orogenic gold deposits: a proposed classification in the context of their crustal distribution and relationship to other gold deposit types. *Ore Geology Reviews* 13, 7–27.
- Hu, R.Z., Bi, X.W., Turner, G., Burnard, P.G., 1999. He and Ar isotope geochemistry studies of gold ore-forming fluids of Ailaoshan gold belt. *Science in China Series D* 29, 321–330 (in Chinese).
- Hu, R.Z., Burnard, P.G., Bi, X.W., Zhou, M.F., Pen, J.T., Su, W.C., Wu, K.X., 2004. Helium and argon isotope geochemistry of alkaline intrusion-associated gold and copper deposits along the Red River–Jinshajiang fault belt, SW China. *Chemical Geology* 203, 305–317.
- Hu, R.Z., Burnard, P.G., Bi, X.W., Zhou, M.F., Pen, J.T., Su, W.C., Zhao, J.H., 2009. Mantle-derived gaseous components in ore-forming fluids of the Xiangshan uranium deposit, Jiangxi province, China: evidence from He, Ar and C isotopes. *Chemical Geology* 266, 86–95.
- Hu, R.Z., Zhou, M.F., 2012. Multiple Mesozoic mineralization events in South China—an introduction to the thematic issue. *Mineralium Deposita* 47, 579–588.
- Hu, S.Q., Zhu, G., Zhang, B.L., Zhang, L., 2010. K–Ar geochronology of the Caledonian event in the Xuefeng uplift. *Geological Review* 56, 490–500 (in Chinese with English abstract).
- Hnatyshin, D., Creaser, R.A., Wilkinson, J.J., Gleeson, S.A., 2015. Re–Os dating of pyrite confirms an early diagenetic onset and extended duration of mineralization in the Irish Zn–Pb ore field. *Geology* 43, 143–146.
- JXBGMR (Bureau of Geology and Mineral Resources of Jiangxi Province), 1984. Regional Geology of the Jiangxi Province. Geol. Publ. House, Beijing, pp. 1–921 (in Chinese with English abstract).
- Kendrick, M.A., Burgess, R., Patrick, R.A.D., Turner, G., 2001. Fluid inclusion noble gas and halogen evidence on the origin of Cu–Porphyry mineralising fluids. *Geochimica et Cosmochimica Acta* 65, 2651–2668.

- Li, D.F., Chen, H.Y., Hollings, P., Zhang, L., Mi, M., Fang, J., Wang, C.M., Lu, W.J., 2016. Re-Os pyrite geochronology of Zn-Pb mineralization in the giant Caixiashan deposit, NW China. *Mineralium Deposita* 51, 309–317.
- Li, H.Q., Wang, D.H., Chen, F.W., Mei, Y.P., Cai, H., 2008. Study on chronology of the Chanziping and daping gold deposit in Xuefeng mountains, Hunan province. *Acta Geologica Sinica* 82, 900–905 (in Chinese with English abstract).
- Li, X.F., Chen, W., Mao, J.W., Wang, C.Z., Xie, G.Q., Feng, Z.H., 2006.  $^{40}\text{Ar}/^{39}\text{Ar}$  dating of sericite from altered dacite porphyry and quartz porphyry in Yinshan polymetallic deposit of Jiangxi Province and its geological significance. *Mineral Deposits* 25, 17–26 (in Chinese with English abstract).
- Li, Y., Li, J.W., Li, X.H., Selby, D., Huang, G.H., Chen, L.J., Zheng, K., 2017a. An Early Cretaceous carbonate replacement origin for the Xinqiao stratabound massive sulfide deposit, Middle-Lower Yangtze Metallogenic Belt, China. *Ore Geology Reviews* 80, 985–1003.
- Li, Y., Selby, D., Condon, D., Tapster, S., 2017b. Cyclic magmatic-hydrothermal evolution in porphyry systems: high-precision U-Pb and Re-Os geochronology constraints from the Tibetan Qulong porphyry Cu-Mo deposit. *Economic Geology* 112, 1419–1440.
- Liu, J.S., 1993. On the mineralization epoch of Xuefeng metallogenetic province. *Gold* 14, 7–12 (in Chinese with English abstract).
- Lu, H.Z., Wang, Z.G., Wu, X.Y., Chen, W.Y., Zhu, X.Q., Guo, D.J., Hu, R.Z., Keita, M., 2005. Turbidite-hosted gold deposits in SE Guizhou province, China: their regional setting, structural control and gold mineralization. *Acta Geologica Sinica* 79, 98–105 (in Chinese with English abstract).
- Lu, H.Z., Wang, Z.G., Chen, W.Y., Wu, X.Y., Zhu, X.Q., Hu, R.Z., 2006. Turbidite hosted gold deposits in southeast Guizhou: their structural control, mineralization characteristics, and some genetic constraints. *Mineral Deposits* 25, 369–387 (in Chinese with English abstract).
- Ludwig, K., 2005. *Isoplot/ex, Version 3.23: a Geochronological Toolkit for Microsoft Excel*. Geochronology Center, Berkeley, USA.
- Luo, X.L., 1989. On the epoch of the formation of Precambrian gold deposits in Hunan province. *Journal of Guilin College of Geology* 9, 25–34 (in Chinese with English abstract).
- Ma, D.S., Pan, J.Y., Xie, Q.L., He, J., 2002. Ore source of Sb (Au) deposits in central Hunan: I. Evidences of trace elements and experimental geochemistry. *Mineral Deposits* 21, 366–376 (in Chinese with English abstract).
- Mao, J.W., Zhang, Z.C., Zhang, Z.H., Du, A.D., 1999. Re-Os isotopic dating of molybdenites in the Xiaoliugou W (Mo) deposit in the northern Qilian Mountains and its geological significance. *Geochimica et Cosmochimica Acta* 63, 1815–1818.
- Mao, J.W., Cheng, Y.B., Cheng, M.H., Pirajno, F., 2013. Major types and time-space distribution of Mesozoic ore deposits in South China and their geodynamic settings. *Mineralium Deposita* 48, 267–294.
- Mathur, R., Ruiz, J., Tornos, F., 1999. Age and sources of the ore at Tharsis and Rio Tinto, Iberian pyrite belt, from Re-Os isotopes. *Mineralium Deposita* 34, 790–793.
- Mikulski, S.Z., Markey, R.J., Stein, H.J., 2005. Re-Os ages for auriferous sulfides from the gold deposits in the Kaczawa Mountains (SW Poland). *Mineral Deposit Research Meeting the Global Challenge Land 2*, 793–796.
- Morelli, R.M., Creaser, R.A., Selby, D., Kelley, K.D., Leach, D.L., King, A.R., 2004. Re-Os sulfide geochronology of the Red Dog sediment-hosted Zn-Pb-Ag deposit, Brooks Range, Alaska. *Economic Geology* 99, 1569–1576.
- Morelli, R.M., Creaser, R.A., Selby, D., Kontak, D.J., Horne, R.J., 2005. Rhenium-Osmium arsenopyrite geochronology of Meguma Group gold deposits, Meguma terrane, Nova Scotia, Canada: evidence for multiple gold mineralizing events. *Economic Geology* 100, 1229–1242.
- Morelli, R.M., Creaser, R.A., Seltmann, F., Stuart, F.M., Selby, D., Graupner, T., 2007. Age and source constraints for the giant Muruntau gold deposit, Uzbekistan, from coupled Re-Os-He isotopes in arsenopyrite. *Geology* 35, 795–798.
- Peng, B., Frei, R., 2004. Nd-Sr-Pb isotopic constraints on metal and fluid sources in W-Sb-Au mineralization at Woxi and Liaojiping (Western Hunan, China). *Mineralium Deposita* 39, 313–327.
- Peng, J.T., Dai, T.G., 1998. On the mineralization epoch of the Xuefeng gold metallogenetic province. *Geology and Prospecting* 34, 37–41 (in Chinese with English abstract).
- Peng, J.T., Dai, T.G., Hu, R.Z., 1999. Geochemical evidence for the ore-forming materials of gold deposits, southwestern Hunan. *Acta Mineralogica Sinica* 19, 327–334 (in Chinese with English abstract).
- Peng, J.T., Hu, R.Z., Zhao, J.H., Fu, Y.Z., Lin, Y.X., 2003. Scheelite Sm-Nd dating and quartz Ar-Ar dating of Au-Sb-W deposit in Woxi, west Hunan. *Chinese Science Bulletin* 48, 1976–1981 (in Chinese).
- Pirajno, F., 2013. *The geology and tectonic settings of China's mineral deposits*. Springer Dordrecht 9–11.
- Ren, J.S., 1996. The continental tectonics of China. *Journal of Southeast Asian Earth Sciences* 13, 197–204.
- Ruiz, J., Mathur, R., 1999. Metallogenesis in continental margins: Re-Os evidence from porphyry copper deposits in Chile. In: Lambert, D., Ruiz, J. (Eds.), *Applications of Radiogenic Isotopes to Ore Deposit Research and Exploration*, vol. 12. Reviews in Economic Geology, pp. 59–72.
- Selby, D., Kelley, K.D., Hitzman, M.W., Zieg, J., 2009. Re-Os Sulfide (bornite, chalcopyrite, and pyrite) systematics of the Carbonate-hosted copper deposits at Ruby Creek, Southern Brooks range, Alaska. *Economic Geology* 104, 437–444.
- Shi, M.K., Fu, B.Q., Jin, X.X., Zhou, X.C., 1993. Antimony Metallogeny in the Central Part of Hunan Province. Hunan Press of Science and Technology, Changsha, pp. 53–65 (in Chinese with English abstract).
- Simmons, S.F., Sawkins, F.J., Schlutter, D.J., 1987. Mantle-derived helium in two Peruvian hydrothermal ore deposits. *Nature* 329, 429–432.
- Shirey, S.B., Walker, R.J., 1998. The Re-Os isotope system in cosmochemistry and high-temperature geochemistry. *Annual Review of Earth and Planetary Sciences* 26, 423–500.
- Smoliar, M.I., Walker, R.J., Morgan, J.W., 1996. Re-Os ages of group IIA, IIIA, IVA, and IVB iron meteorites. *Science* 271, 1099–1102.
- Stein, H.J., Sundblad, K., Markey, R.J., Morgan, J.W., Motuza, G., 1998. Re-Os ages for Archean molybdenite and pyrite, Kuitila-Kivisuo, Finland, and Proterozoic molybdenite, Kabeliai, Lithuania: testing the chronometer in a metamorphic and metasomatic setting. *Mineralium Deposita* 33, 329–345.
- Stein, H.J., Morgan, J.W., Schersten, A., 2000. Re-Os dating of low-level highly radiogenic (LLHR) sulfides: the Harnas gold deposit, southwest Sweden, Records continental scale tectonic events. *Economic Geology* 95, 1657–1671.
- Stuart, F.M., Turner, G., Duckworth, R.C., Fallick, A.E., 1994. Helium isotopes as tracers of trapped hydrothermal fluids in ocean-floor sulfides. *Geology* 22, 823–826.
- Stuart, F.M., Burnard, P.G., Taylor, R.P., Turner, G., 1995. Resolving mantle and crustal contributions to ancient hydrothermal fluids: He-Ar isotopes in fluid inclusions from Dae Hwa W-Mo mineralisation, South Korea. *Geochimica et Cosmochimica Acta* 59, 4663–4673.
- Suzuki, K., Kagi, H., Nara, M., Takano, B., Nozaki, Y., 2000. Experimental alteration of molybdenite: evaluation of the Re-Os system, infrared spectroscopic profile and polypeptide. *Geochim Cosmochim Acta* 64, 223–232.
- Wang, J.S., 2012. *Mineralization, Geochronology and Geodynamics of the Low-temperature Epithermal Metallogenic Domain in Southwestern China*. Doctorate Dissertation of Graduate University of Chinese Academy of Sciences, pp. 81–84 (in Chinese with English abstract).
- Wang, Y.J., Zhang, Y.H., Fan, W.M., Peng, T.P., 2005. Structural signatures and  $^{40}\text{Ar}/^{39}\text{Ar}$  geochronology of the Indosinian Xuefengshan tectonic belt, south China block. *Journal of Structural Geology* 27, 985–998.
- Wang, Y.J., Fan, W.M., Zhao, G.C., Ji, S.C., Peng, T.P., 2007. Zircon U–Pb geochronology of gneissic rocks in the Yunkai massif and its implications on the Caledonian event in the South China block. *Gondwana Research* 12, 404–416.
- Wang, X.Z., Liang, H.Y., Shan, Q., Cheng, J.P., Xia, P., 1999. Metallogenic age of the Jinshan gold deposit and Caledonian gold mineralization in South China. *Geological Review* 45, 19–25 (in Chinese with English abstract).
- Windh, J., 1995. Saddle reef and related gold mineralization, Hill End gold field, Australia: evolution of an auriferous vein system during progressive deformation. *Economic Geology* 90, 1764–1775.
- Wu, L.Y., Hu, R.Z., Peng, J.T., Bi, X.W., Jiang, G.H., Chen, H.W., Wang, Q.Y., Liu, Y.Y., 2011. He and Ar isotopic compositions and genetic implications for the giant Shizhuyuan W–Sn–Bi–Mo deposit, Hunan Province, South China. *International Geology Review* 53, 677–690.
- Xue, H.M., Ma, F., Song, Y.Q., Xie, Y.P., 2010. Geochronology and geochemistry of the Neoproterozoic granitoid association from eastern segment of the Jiangnan orogen, China: constraints on the timing and process of amalgamation between the Yangtze and Cathaysia blocks. *Acta Petrologica Sinica* 26, 3215–3244 (in Chinese with English abstract).
- Ye, X.R., Wu, M.B., Sun, M.L., 2001. Determination of the noble gas isotopic composition in rocks and minerals by Mass Spectrometry. *Rock and Mineral Analysis* 20, 174–178 (in Chinese with English abstract).
- Zhang, L.C., Xiao, W.J., Qin, K.Z., Qu, W.J., Du, A.D., 2005. Re-Os isotopic dating of molybdenite and pyrite in the Baishan Mo-Re deposit, eastern Tianshan, NW China, and its geological significance. *Mineralium Deposita* 39, 960–969.
- Zhao, J.H., Peng, J.T., Hu, R.Z., Fu, Y.Z., 2005. Chronology, petrology, geochemistry and tectonic environment of Banxi quartz porphyry dikes, Hunan province. *Acta Geoscientia Sinica* 26, 525–534 (in Chinese with English abstract).
- Zhou, T.H., Goldfarb, R.J., Phillips, G.N., 2002. Tectonics and distribution of gold deposits in China – an overview. *Mineralium Deposita* 37, 249–282.
- Zhu, X.Q., Wang, G.L., Lu, H.Z., Wu, X.Y., Chen, W.Y., 2006. Determination of the age of gold deposits in southeastern Guizhou: with a discussion of the Caledonian Hunan–Guizhou gold ore belt. *Geology in China* 33, 1092–1099 (in Chinese with English abstract).
- Zhu, Y.N., Peng, J.T., 2015. Infrared microthermometric and noble gas isotope study of fluid inclusions in ore minerals at the Woxi orogenic Au-Sb-W deposit, western Hunan, South China. *Ore Geology Reviews* 65, 55–69.